

1      **MitoChime: A Machine-Learning Pipeline for**  
2      **Detecting PCR-Induced Chimeras in**  
3      **Mitochondrial Illumina Reads**

4                          A Special Project Proposal  
5                          Presented to  
6                          the Faculty of the Division of Physical Sciences and Mathematics  
7                          College of Arts and Sciences  
8                          University of the Philippines Visayas  
9                          Miag-ao, Iloilo

10                         In Partial Fulfillment  
11                         of the Requirements for the Degree of  
12                         Bachelor of Science in Computer Science

13                         by

14                         Duranne Duran  
15                         Yvonne Lin  
16                         Daniella Pailden

17                         Adviser  
18                         Francis Dimzon

19                         November 25, 2025

# **Contents**

21	<b>1 Introduction</b>	1
22	1.1 Overview . . . . .	1
23	1.2 Problem Statement . . . . .	3
24	1.3 Research Objectives . . . . .	4
25	1.3.1 General Objective . . . . .	4
26	1.3.2 Specific Objectives . . . . .	4
27	1.4 Scope and Limitations of the Research . . . . .	5
28	1.5 Significance of the Research . . . . .	6
29	<b>2 Review of Related Literature</b>	7
30	2.1 The Mitochondrial Genome . . . . .	7
31	2.1.1 Mitochondrial Genome Assembly . . . . .	8

32	2.2 PCR Amplification and Chimera Formation . . . . .	9
33	2.2.1 Effects of Chimeric Reads on Organelle Genome Assembly	10
34	2.3 Existing Traditional Approaches for Chimera Detection . . . . .	11
35	2.3.1 UCHIME . . . . .	12
36	2.3.2 UCHIME2 . . . . .	14
37	2.3.3 CATch . . . . .	16
38	2.3.4 ChimPipe . . . . .	17
39	2.4 Machine Learning Approaches for Chimera and Sequence Quality	
40	Detection . . . . .	18
41	2.4.1 Feature-Based Representations of Genomic Sequences . . .	18
42	2.5 Synthesis of Chimera Detection Approaches . . . . .	20
43	<b>3 Research Methodology</b>	<b>25</b>
44	3.1 Research Activities . . . . .	25
45	3.1.1 Data Collection . . . . .	26
46	3.1.2 Data Simulation . . . . .	27
47	3.1.3 Bioinformatics Tools Pipeline . . . . .	28
48	3.1.4 Machine-Learning Model Development . . . . .	31

49	3.1.5 Validation and Testing . . . . .	32
50	3.1.6 Documentation . . . . .	32
51	3.2 Calendar of Activities . . . . .	33

# <sup>52</sup> List of Figures

<sup>53</sup>	3.1 Process Diagram of Special Project . . . . .	26
---------------	--	----

## 54 List of Tables

<sup>57</sup> **Chapter 1**

<sup>58</sup> **Introduction**

<sup>59</sup> **1.1 Overview**

<sup>60</sup> The rapid advancement of next-generation sequencing (NGS) technologies has  
<sup>61</sup> transformed genomic research by enabling high-throughput and cost-effective  
<sup>62</sup> DNA analysis (Metzker, 2010). Among current platforms, Illumina sequencing  
<sup>63</sup> remains the most widely adopted, capable of producing millions of short reads  
<sup>64</sup> that can be assembled into reference genomes or analyzed for genetic variation  
<sup>65</sup> (Bentley et al., 2008; Glenn, 2011). Despite its high base-calling accuracy,  
<sup>66</sup> Illumina sequencing is prone to artifacts introduced during library preparation,  
<sup>67</sup> particularly polymerase chain reaction (PCR)-induced chimeras, which are ar-  
<sup>68</sup> tificial hybrid sequences that do not exist in the true genome (Judo, Wedel, &  
<sup>69</sup> Wilson, 1998).

<sup>70</sup> PCR chimeras form when incomplete extension products from one template

71 anneal to an unrelated DNA fragment and are extended, creating recombinant  
72 reads (Qiu et al., 2001). In mitochondrial genome assembly, such artifacts are  
73 especially problematic because the mitochondrial genome is small, circular, and  
74 often repetitive (Boore, 1999; Cameron, 2014). Even a small number of chimeric  
75 or mis-joined reads can reduce assembly contiguity and introduce false junctions  
76 during organelle genome reconstruction (Dierckxsens, Mardulyn, & Smits, 2017;  
77 Hahn, Bachmann, & Chevreux, 2013; Jin et al., 2020). Existing assembly tools  
78 such as GetOrganelle and MITObim assume that input reads are largely free of  
79 such artifacts (Hahn et al., 2013; Jin et al., 2020). Consequently, undetected  
80 chimeras may produce fragmented assemblies or misidentified organellar bound-  
81 aries. To ensure accurate reconstruction of mitochondrial genomes, a reliable  
82 and automated method for detecting and filtering PCR-induced chimeras before  
83 assembly is essential.

84 This study focuses on mitochondrial sequencing data from the genus *Sar-*  
85 *dinella*, a group of small pelagic fishes widely distributed in Philippine waters.  
86 Among them, *Sardinella lemuru* (Bali sardinella) is one of the country's most  
87 abundant and economically important species, providing protein and livelihood  
88 to coastal communities (Labrador, Agmata, Palermo, Ravago-Gotanco, & Pante,  
89 2021; Willette, Bognot, Mutia, & Santos, 2011). Accurate mitochondrial assem-  
90 blies are critical for understanding its population genetics, stock structure, and  
91 evolutionary history. However, assembly pipelines often encounter errors or fail  
92 to complete due to undetected chimeric reads. To address this gap, this research  
93 introduces **MitoChime**, a machine-learning pipeline designed to detect and filter  
94 PCR-induced chimeric reads using both alignment- and sequence-derived statisti-  
95 cal features. The tool aims to provide bioinformatics laboratories, particularly the

<sub>96</sub> Philippine Genome Center Visayas, with an efficient, interpretable, and resource-  
<sub>97</sub> optimized solution for improving mitochondrial genome reconstruction.

## <sub>98</sub> 1.2 Problem Statement

<sub>99</sub> While NGS technologies have revolutionized genomic data acquisition, the ac-  
<sub>100</sub> curacy of mitochondrial genome assembly remains limited by artifacts produced  
<sub>101</sub> during PCR amplification. These chimeric reads can distort assembly graphs and  
<sub>102</sub> cause misassemblies, with especially severe effects in small, circular mitochon-  
<sub>103</sub> drial genomes (Boore, 1999; Cameron, 2014). Existing assembly pipelines such  
<sub>104</sub> as GetOrganelle, MITObim, and NOVOPlasty assume that sequencing reads are  
<sub>105</sub> free of such artifacts (Dierckxsens et al., 2017; Hahn et al., 2013; Jin et al., 2020).  
<sub>106</sub> At the Philippine Genome Center Visayas, several mitochondrial assemblies have  
<sub>107</sub> failed or yielded incomplete contigs despite sufficient coverage, suggesting that  
<sub>108</sub> undetected chimeric reads compromise assembly reliability. Meanwhile, exist-  
<sub>109</sub> ing chimera-detection tools such as UCHIME and VSEARCH were developed  
<sub>110</sub> primarily for amplicon-based microbial community analysis and rely heavily on  
<sub>111</sub> reference or taxonomic comparisons (Edgar, Haas, Clemente, Quince, & Knight,  
<sub>112</sub> 2011; Rognes, Flouri, Nichols, Quince, & Mahé, 2016). These approaches are un-  
<sub>113</sub> suitable for single-species organellar data, where complete reference genomes are  
<sub>114</sub> often unavailable. Therefore, there is a pressing need for a reference-independent,  
<sub>115</sub> data-driven tool capable of automatically detecting and filtering PCR-induced  
<sub>116</sub> chimeras in mitochondrial sequencing datasets.

<sub>117</sub> **1.3 Research Objectives**

<sub>118</sub> **1.3.1 General Objective**

<sub>119</sub> To develop and evaluate a machine-learning-based pipeline (MitoChime) capable  
<sub>120</sub> of detecting PCR-induced chimeric reads in *Sardinella* mitochondrial sequencing  
<sub>121</sub> data to improve the accuracy of mitochondrial genome assembly.

<sub>122</sub> **1.3.2 Specific Objectives**

<sub>123</sub> Specifically, the researchers aim to:

- <sub>124</sub> 1. Construct empirical as well as simulated *Sardinella* Illumina paired-end  
<sub>125</sub> datasets containing both clean and PCR-induced chimeric reads.
- <sub>126</sub> 2. Extract alignment and sequence-based features such as k-mer composition,  
<sub>127</sub> junction complexity, split-alignment counts from both clean and chimeric  
<sub>128</sub> reads.
- <sub>129</sub> 3. Train, validate, and compare supervised machine-learning models for classi-  
<sub>130</sub> fying reads as clean or chimeric.
- <sub>131</sub> 4. Determine feature importance and identify the most informative indicators  
<sub>132</sub> of PCR-induced chimerism.
- <sub>133</sub> 5. Integrate the optimized classifier into a modular and interpretable pipeline  
<sub>134</sub> deployable on standard computing environments at PGC Visayas.

## 135 1.4 Scope and Limitations of the Research

136 This study focuses on detecting PCR-induced chimeric reads in Illumina paired-  
137 end mitochondrial sequencing data from the *Sardinella lemuru* species. The deci-  
138 sion to limit the taxonomic scope is motivated by three factors: (1) To provide a  
139 biologically coherent system by eliminating interspecific variation, such as differ-  
140 ences in mitochondrial genome size, GC content, and repetitive regions. Restrict-  
141 ing the analysis to *S. lemuru* reduces biological noise and ensures that observed  
142 patterns reflect chimeric artifacts rather than taxonomic differences. (2) The se-  
143 lected species is directly relevant to ongoing research initiatives and sequencing  
144 efforts at the Philippine Genome Center Visayas, making it a strategically ap-  
145 propriate choice for developing and validating the analytical framework; and (3)  
146 *Sardinella lemuru* possesses a moderately complex but well-characterized mito-  
147 chondrial genome, with clear gene boundaries and sufficient publicly available  
148 data from repositories such as the National Center for Biotechnology Information  
149 (NCBI).

150 The study emphasizes `wgsim`-based simulations and selected empirical mito-  
151 chondrial datasets. It excludes naturally occurring chimeras, nuclear mitochon-  
152 drial pseudogenes (NUMTs), and large-scale structural rearrangements in nuclear  
153 genomes. Feature extraction prioritizes interpretable, shallow statistics and align-  
154 ment metrics rather than deep-learning embeddings to ensure transparency and  
155 computational efficiency. Testing on long-read platforms (e.g., Nanopore, PacBio)  
156 and other taxa lies beyond the project's scope. The resulting pipeline will serve  
157 as a foundation for future, broader chimera-detection frameworks applicable to  
158 diverse organellar genomes.

## <sup>159</sup> 1.5 Significance of the Research

<sup>160</sup> This research provides both methodological and practical contributions to mi-  
<sup>161</sup>tochondrial genomics and bioinformatics. First, MitoChime enhances assembly  
<sup>162</sup>accuracy by filtering PCR-induced chimeras prior to genome assembly, thereby  
<sup>163</sup>improving the contiguity and correctness of *Sardinella* mitochondrial genomes.  
<sup>164</sup> Second, it promotes automation and reproducibility by replacing subjective man-  
<sup>165</sup>ual curation with a data-driven, machine-learning-based workflow. Third, the  
<sup>166</sup>pipeline demonstrates computational efficiency through its design, enabling im-  
<sup>167</sup>plementation on modest computing infrastructures commonly available in regional  
<sup>168</sup>laboratories. Beyond technical improvements, MitoChime contributes to local ca-  
<sup>169</sup>pacity building by strengthening expertise in bioinformatics and machine-learning  
<sup>170</sup>integration, aligning with the mission of the Philippine Genome Center Visayas.  
<sup>171</sup> Finally, accurate mitochondrial assemblies are vital for fisheries management,  
<sup>172</sup>population genetics, and biodiversity conservation, providing reliable genomic re-  
<sup>173</sup>sources for species such as *Sardinella*. Through these contributions, MitoChime  
<sup>174</sup>advances the reliability of mitochondrial genome reconstruction and supports sus-  
<sup>175</sup>tainable, data-driven research in Philippine genomics.

<sup>176</sup> **Chapter 2**

<sup>177</sup> **Review of Related Literature**

<sup>178</sup> This chapter presents an overview of the literature relevant to the study. It  
<sup>179</sup> discusses the biological and computational foundations underlying mitochondrial  
<sup>180</sup> genome analysis and assembly, as well as existing tools, algorithms, and techniques  
<sup>181</sup> related to chimera detection and genome quality assessment. The chapter aims to  
<sup>182</sup> highlight the strengths, limitations, and research gaps in current approaches that  
<sup>183</sup> motivate the development of the present study.

<sup>184</sup> **2.1 The Mitochondrial Genome**

<sup>185</sup> Mitochondrial genome (mtDNA) is a small, typically circular molecule found in  
<sup>186</sup> most eukaryotes. It encodes essential genes involved in oxidative phosphorylation  
<sup>187</sup> and energy metabolism. Because of its conserved structure and maternal inher-  
<sup>188</sup> itance, mtDNA has become a valuable genetic marker for studies in evolution,  
<sup>189</sup> population genetics, and phylogenetics (Anderson et al., 1981; Boore, 1999). In

190 animal species, the mitochondrial genome ranges from 15–20 kilobase and contains  
191 13 protein-coding genes, 22 tRNAs, and two rRNAs arranged compactly without  
192 introns (Gray, 2012). In comparison to nuclear DNA the ratio of the number  
193 of copies of mtDNA is higher and has relatively simple organization which make  
194 it particularly suitable for genome sequencing and assembly studies (Dierckxsens  
195 et al., 2017). Moreover, mitochondrial genomes provide crucial insights into evo-  
196 lutionary relationships among species and are increasingly used for testing new  
197 genomic assembly and analysis methods.

### 198 **2.1.1 Mitochondrial Genome Assembly**

199 Mitochondrial genome assembly refers to the reconstruction of the complete mito-  
200 chondrial DNA (mtDNA) sequence from raw or fragmented sequencing reads. It is  
201 conducted to obtain high-quality, continuous representations of the mitochondrial  
202 genome that can be used for a wide range of analyses, including species identi-  
203 fication, phylogenetic reconstruction, evolutionary studies, and investigations of  
204 mitochondrial diseases. Because mtDNA evolves relatively rapidly and is mater-  
205 nally inherited, its assembled sequence provides valuable insights into population  
206 structure, lineage divergence, and adaptive evolution across taxa (Boore, 1999).  
207 Compared to nuclear genome assembly, assembling the mitochondrial genome is  
208 often considered more straightforward but still encounters distinct technical chal-  
209 lenges such as sequencing errors, low coverage regions, and chimeric reads that can  
210 distort the final assembly, leading to incomplete or misassembled genomes. These  
211 errors can propagate into downstream analyses, emphasizing the need for robust  
212 chimera detection and sequence validation methods in mitochondrial genome re-

213 search.

## 214 2.2 PCR Amplification and Chimera Formation

215 Polymerase Chain Reaction (PCR) plays an important role in next-generation  
216 sequencing (NGS) library preparation, as it amplifies target DNA fragments for  
217 downstream analysis. However, the amplification process can also introduce arti-  
218 facts that affect data accuracy, one of them being the formation of chimeric se-  
219 quences. Chimeras typically arise when incomplete extension occurs during a PCR  
220 cycle. This causes the DNA polymerase to switch from one template to another  
221 and generate hybrid recombinant molecules (Judo et al., 1998). Artificial chimeras  
222 are produced through such amplification errors, whereas biological chimeras oc-  
223 cur naturally through genomic rearrangements or transcriptional events. These  
224 biological chimeras can have functional roles and may encode tissue-specific novel  
225 proteins that link to cellular processes or diseases (Frenkel-Morgenstern et al.,  
226 2012).

227 In the context of amplicon-based sequencing, PCR-induced chimeras can sig-  
228 nificantly distort analytical outcomes. Their presence artificially inflates estimates  
229 of genetic or microbial diversity and may cause misassemblies during genome re-  
230 construction. (Qin et al., 2023) has reported that chimeric sequences may account  
231 for more than 10% of raw reads in amplicon datasets. This artifact tends to be  
232 most prominent among rare operational taxonomic units (OTUs) or singletons,  
233 which are sometimes misinterpreted as novel diversity, which further causes the  
234 complication of microbial diversity analyses (Gonzalez, Zimmermann, & Saiz-

235 Jimenez, 2004). Moreover, the likelihood of chimera formation has been found to  
236 vary with the GC content of target sequences, with lower GC content generally  
237 associated with a reduced rate of chimera generation (Qin et al., 2023).

238 **2.2.1 Effects of Chimeric Reads on Organelle Genome As-**  
239 **sembly**

240 In mitochondrial DNA (mtDNA) assembly workflows, PCR-induced chimeras pose  
241 additional challenges. Assembly tools such as GetOrganelle and MitoBeam, which  
242 operate under the assumption of organelle genome circularity, are vulnerable when  
243 chimeric reads disrupt this circular structure. Such disruptions can lead to assem-  
244 bly errors or misassemblies (Bi et al., 2024). These artificial sequences interfere  
245 with the assembly graph, which makes it more difficult to accurately reconstruct  
246 mitochondrial genomes. In addition, these artifacts propagate false variants and  
247 erroneous annotations in genomic data. Hence, determining and minimizing PCR-  
248 induced chimera formation is vital for improving the quality of mitochondrial  
249 genome assemblies, and ensuring the reliability of amplicon sequencing data.

250    **2.3 Existing Traditional Approaches for Chimera**  
251    **Detection**

252    Several computational tools have been developed to identify chimeric sequences in  
253    NGS datasets. These tools generally fall into two categories: reference-based and  
254    de novo approaches. Reference-based chimera detection, also known as database-  
255    dependent detection, is one of the earliest and most widely used computational  
256    strategies for identifying chimeric sequences in amplicon-based microbial commu-  
257    nity studies. These methods rely on the comparison of each query sequence against  
258    a curated, high-quality database of known, non-chimeric reference sequences to  
259    determine whether the query can be more plausibly explained as a composite or  
260    a mosaic of two or more reference sequences rather than as a genuine biological  
261    variant (Edgar et al., 2011).

262    On the other hand, the De novo chimera detection, also referred to as reference-  
263    free detection, represents an alternative computational paradigm that identifies  
264    chimeric sequences without reliance on external reference databases. Instead of  
265    comparing each query sequence to a curated collection of known, non-chimeric  
266    sequences, de novo methods infer chimeras based on internal relationships among  
267    the sequences present within the dataset itself. This approach is particularly  
268    advantageous in studies of novel, under explored, or taxonomically diverse mi-  
269    crobial communities where comprehensive reference databases are unavailable or  
270    incomplete (Edgar, 2016; Edgar et al., 2011). The underlying assumption on this  
271    method operates on the key biological principle that true biological sequences are  
272    generally more abundant than chimeric artifacts. During PCR amplification, au-  
273    thentic sequences are amplified early and tend to dominate the read pool, while

274 chimeric sequences form later resulting in the tendency to appear at lower relative  
275 abundances compared to their true parental sequences. As such, the abundance  
276 hierarchy is formed by treating the most abundant sequences as supposed parents  
277 and testing whether less abundant sequences can be reconstructed as mosaics of  
278 these dominant templates. In addition to abundance, de novo algorithms assess  
279 compositional and structural similarity among sequences, examining whether cer-  
280 tain regions of a candidate sequence align more closely with one high-abundance  
281 sequence and other regions with a different one.

282 Both reference-based and de novo approaches are complementary rather than  
283 mutually exclusive. Reference-based methods provide stability and reproducibility  
284 when curated databases are available, whereas de novo methods offer flexibility  
285 and independence for novel or highly diverse communities. In practice, many  
286 modern bioinformatics pipelines combine both paradigms sequentially: an initial  
287 de novo step identifies dataset-specific chimeras, followed by a reference-based pass  
288 that removes remaining artifacts relative to established databases (Edgar, 2016).  
289 These two methods of detection form the foundation of tools such as UCHIME  
290 and later UCHIME2, exemplified by the dual capability of providing both modes  
291 within a unified computational framework.

### 292 **2.3.1 UCHIME**

293 Developed by Edgar et al. (Edgar et al., 2011), UCHIME is one of the most widely  
294 used computational tools for detecting chimeric sequences in amplicon sequencing  
295 data. The UCHIME algorithm detects chimeras by evaluating how well a query  
296 sequence ( $Q$ ) can be explained as a mosaic of two parent sequences (A and B)

297 from a reference database. The query sequence is first divided into four non-  
298 overlapping segments or chunks. Each chunk is independently searched against a  
299 reference database that is assumed to be free of chimeras. The best matches to  
300 each segment are collected, and from these results, two candidate parent sequences  
301 are identified, typically the two sequences that best explain all chunks of the query.  
302 Then a three-way alignment among the query (Q) and the two parent candidates  
303 (A and B) is done. From this alignment, UCHIME attempts to find a chimeric  
304 model (M) which is a hypothetical recombinant sequence formed by concatenating  
305 fragments from A and B that best match the observed Q

### 306 Chimeric Alignment and Scoring

307 To decide whether a query is chimeric, UCHIME computes several alignment-  
308 based metrics between Q, its top hit (T, the most similar known sequence), and  
309 the chimeric model (M). The key differences are measured as: dQT or the number  
310 of mismatches between the query and the top hit as well as dQM or the number  
311 of mismatches between the query and the chimeric model. From these, a chimera  
312 score is calculated to quantify how much better the chimeric model fits the query  
313 compared to a single parent. If the model's similarity to Q exceeds a defined  
314 threshold (typically  $\geq 0.8\%$  better identity), the sequence is reported as chimeric.  
315 A higher score indicates stronger evidence of chimerism, while lower scores suggest  
316 that the sequence is more likely to be authentic.

317 In de novo mode, UCHIME applies an abundance-driven strategy. Only se-  
318 quences at least twice as abundant as the query are considered as potential parents.  
319 Non-chimeric sequences identified at each step are added iteratively to a growing

320 internal database for subsequent queries.

### 321 **Limitations of UCHIME**

322 Although UCHIME was a significant advancement in chimera detection, it has  
323 notable limitations. According to (Edgar, 2016) and the UCHIME practical notes  
324 (Edgar, n.d), many of the accuracy results reported in the original 2011 paper  
325 were overly optimistic due to unrealistic benchmark designs that assumed com-  
326 plete reference coverage and perfect sequence quality. In practice, UCHIME's  
327 accuracy can decline when: (1) The reference database is incomplete or contains  
328 erroneous entries. (2) Low-divergence chimeras are present, as these closely resem-  
329 ble genuine biological variants. (3) Sequence datasets include residual sequencing  
330 errors, leading to spurious alignments or misidentification; and (4) The abundance  
331 ratio between parent and chimera is distorted by amplification bias. Additionally,  
332 UCHIME tends to misclassify sequences as non-chimeric when parent sequences  
333 are missing from the database. These limitations motivated the development of  
334 UCHIME2.

### 335 **2.3.2 UCHIME2**

336 To overcome the limitations of its predecessor, UCHIME2 (Edgar, 2016) intro-  
337 duced several methodological and algorithmic refinements that significantly en-  
338 hanced the accuracy and reliability of chimera detection. One major improve-  
339 ment lies in its approach to uncertainty handling. In earlier versions, sequences  
340 with limited reference support were often incorrectly classified as non-chimeric,

341 increasing the likelihood of false negatives. UCHIME2 addresses this issue by  
342 designating such ambiguous sequences as “unknown,” thereby providing a more  
343 conservative and reliable classification framework.

344 Another notable advancement is the introduction of multiple application-  
345 specific modes that allow users to tailor the algorithm’s performance to the  
346 characteristics of their datasets. The following parameter presets: denoised,  
347 balanced, sensitive, specific, and high-confidence, enable researchers to optimize  
348 the balance between sensitivity and specificity according to the goals of their  
349 analysis.

350 In comparative evaluations, UCHIME2 demonstrated superior detection per-  
351 formance, achieving sensitivity levels between 93% and 99% and lower overall  
352 error rates than earlier versions or other contemporary tools such as DECIPHER  
353 and ChimeraSlayer. Despite these advances, the study also acknowledged a fun-  
354 damental limitation in chimera detection: complete error-free identification is  
355 theoretically unattainable. This is due to the presence of “perfect fake models,”  
356 wherein genuine non-chimeric sequences can be perfectly reconstructed from other  
357 reference fragments. This underscore the uncertainty in differentiating authentic  
358 biological sequences from artificial recombinants based solely on sequence similar-  
359 ity, emphasizing the need for continued methodological refinement and cautious  
360 interpretation of results.

361 **2.3.3 CATch**

362 Early chimera detection programs such as UCHIME (Edgar et al., 2011) relied on  
363 alignment-based and abundance-based heuristics to identify hybrid sequences in  
364 amplicon data. However, researchers soon observed that different algorithms often  
365 produced inconsistent predictions. A sequence might be identified as chimeric by  
366 one tool but classified as non-chimeric by another, resulting in unreliable filtering  
367 outcomes across studies.

368 To address these inconsistencies, (Mysara, Saeys, Leys, Raes, & Monsieurs,  
369 2015) developed the Classifier for Amplicon Tool Chimeras (CATCh), which rep-  
370 resents the first ensemble machine learning system designed for chimera detection  
371 in 16S rRNA amplicon sequencing. Rather than depending on a single detec-  
372 tion strategy, CATCh integrates the outputs of several established tools, includ-  
373 ing UCHIME, ChimeraSlayer, DECIPHER, Pintail, and Perseus. The individual  
374 scores and binary decisions generated by these tools are used as input features for  
375 a supervised learning model. The algorithm employs a Support Vector Machine  
376 (SVM) with a Pearson VII Universal Kernel (PUK) to determine optimal weight-  
377 ings among the input features and to assign each sequence a probability of being  
378 chimeric.

379 Benchmarking in both reference-based and de novo modes demonstrated signif-  
380 icant performance improvements. CATCh achieved sensitivities of approximately  
381 85 percent in reference-based mode and 92 percent in de novo mode, with corre-  
382 sponding specificities of approximately 96 percent and 95 percent. These results  
383 indicate that CATCh detected 7 to 12 percent more chimeras than any individual  
384 algorithm while maintaining high precision. Integration of CATCh into amplicon-

385 processing pipelines also reduced operational taxonomic unit (OTU) inflation by  
386 23 to 35 percent, producing diversity estimates that more closely reflected true  
387 community composition.

### 388 2.3.4 ChimPipe

389 Among the available tools for chimera detection, ChimPipe is a bioinformatics  
390 pipeline developed to identify chimeric sequences such as fusion genes and  
391 transcription-induced chimeras from paired-end RNA sequencing data. It uses  
392 both discordant paired-end reads and split-read alignments to improve the ac-  
393 curacy and sensitivity of detecting fusion genes, trans-splicing events, and read-  
394 through transcripts (Rodriguez-Martin et al., 2017). By combining these two  
395 sources of information, ChimPipe achieves better precision than methods that  
396 depend on a single type of signal.

397 The pipeline works with many eukaryotic species that have available genome  
398 and annotation data, making it a versatile tool for studying chimera evolution  
399 and transcriptome structure (Rodriguez-Martin et al., 2017). It can also predict  
400 multiple isoforms for each gene pair and identify breakpoint coordinates that are  
401 useful for reconstructing and verifying chimeric transcripts. Tests using both  
402 simulated and real datasets have shown that ChimPipe maintains high accuracy  
403 and reliable performance.

404 ChimPipe’s modular design lets users adjust parameters to fit different se-  
405 quencing protocols or organism characteristics. Experimental results have con-  
406 firmed that many chimeric transcripts detected by the tool correspond to func-

407 tional fusion proteins, showing its value for understanding chimera biology and  
408 its potential applications in disease research (Rodriguez-Martin et al., 2017).

## 409 **2.4 Machine Learning Approaches for Chimera 410 and Sequence Quality Detection**

411 Traditional chimera detection tools rely primarily on heuristic or alignment-based  
412 rules. Recent advances in machine learning (ML) have demonstrated that mod-  
413 els trained on sequence-derived features can effectively capture compositional and  
414 structural patterns in biological sequences. Although most existing ML systems  
415 such as those used for antibiotic resistance prediction, taxonomic classification,  
416 or viral identification are not specifically designed for chimera detection, they  
417 highlight how data-driven models can outperform similarity-based heuristics by  
418 learning intrinsic sequence signatures. In principle, ML frameworks can inte-  
419 grate diverse indicators such as k-mer frequencies, GC-content variation, and  
420 split-alignment metrics to identify subtle anomalies that may indicate a chimeric  
421 origin (Arango et al., 2018; Liang, Bible, Liu, Zou, & Wei, 2020; Ren et al., 2020).

### 422 **2.4.1 Feature-Based Representations of Genomic Se- 423 quences**

424 In genomic analysis, feature extraction converts DNA sequences into numerical  
425 representations suitable for ML algorithms. A common approach is k-mer fre-  
426 quency analysis, where normalized k-mer counts form the feature vector (Vervier,

427 2015). These features effectively capture local compositional patterns that often  
428 differ between authentic and chimeric reads. In particular, deviations in k-mer  
429 profiles between adjacent read segments can serve as a compositional signature  
430 of template-switching events. Additional descriptors such as GC content and  
431 sequence entropy can further distinguish sequence types; in metagenomic classifi-  
432 cation and virus detection, k-mer-based features have shown strong performance  
433 and robustness to noise (Ren et al., 2020; Vervier, 2015). For chimera detection  
434 specifically, abrupt shifts in GC or k-mer composition along a read can indicate  
435 junctions between parental fragments. Windowed feature extraction enables mod-  
436 els to capture these discontinuities that rule-based algorithms may overlook.

437 Machine learning models can also leverage alignment-derived features such as  
438 the frequency of split alignments, variation in mapping quality, and local cover-  
439 age irregularities. Split reads and discordant read pairs are classical signatures  
440 of genomic junctions and have been formalized in probabilistic frameworks for  
441 structural-variant discovery that integrate multiple evidence types (Layer, Hall, &  
442 Quinlan, 2014). Similarly, long-read tools such as Sniffles employ split-alignment  
443 and coverage anomalies to accurately localize breakpoints (Sedlazeck et al., 2018).  
444 Modern aligners such as Minimap2 (Li, 2018) output supplementary (SA tags) and  
445 secondary alignments as well as chaining and alignment-score statistics that can  
446 be summarized into quantitative predictors for machine-learning models. These  
447 alignment-signal features are particularly relevant to PCR-induced mitochondrial  
448 chimeras, where template-switching events produce reads partially matching dis-  
449 tinct regions of the same or related genomes. Integrating such cues within a  
450 supervised-learning framework enables artifact detection even in datasets lacking  
451 complete or perfectly assembled references.

452 A further biologically grounded descriptor is micro-homology length at puta-  
453 tive junctions. Micro-homology refers to short, shared sequences (often in the  
454 range of a few to tens of base pairs) that are near breakpoints and mediate  
455 non-canonical repair or template-switch mechanisms. Studies of double strand  
456 break repair and structural variation have demonstrated that the length of micro-  
457 homology correlates with the likelihood of micro-homology-mediated end joining  
458 (MMEJ) or fork-stalled template-switching pathways (Sfeir & Symington, 2015).  
459 In the context of PCR-induced chimeras, template switching during amplifica-  
460 tion often leaves short identical sequences at the junction of two concatenated  
461 fragments. Quantifying the longest exact suffix–prefix overlap at each candidate  
462 breakpoint thus provides a mechanistic signature of chimerism and complements  
463 both compositional (k-mer) and alignment (SA count) features.

## 464 2.5 Synthesis of Chimera Detection Approaches

465 To provide an integrated overview of the literature discussed in this chapter, Ta-  
466 ble 2.1 summarizes the major chimera detection studies, their methodological  
467 approaches, and their known limitations. This consolidated comparison brings to-  
468 gether reference-based approaches, de novo strategies, alignment-driven tools, en-  
469 semble machine-learning systems, and general ML-based sequence-quality frame-  
470 works. Presenting these methods side-by-side clarifies their performance bound-  
471 aries and highlights the unresolved challenges that persist in mitochondrial genome  
472 analysis and chimera detection.

Table 2.1: Summary of Existing Methods and Research

## Gaps

<b>Method/Study</b>	<b>Scope/Approach</b>	<b>Limitations</b>
Reference-based Chimera Detection	Compares query sequences against curated, non-chimeric reference databases; identifies mosaic sequences by evaluating similarity to known templates.	Depends heavily on completeness and quality of reference databases; often fails when novel taxa or missing parent sequences are present; reduced accuracy for low-divergence chimeras.
De novo Chimera Detection	Identifies chimeras using only internal dataset relationships; relies on abundance patterns and compositional similarity; reconstructs sequences as mosaics of high-abundance parents.	Assumes true sequences are more abundant—fails when amplification bias distorts abundance; struggles with evenly abundant parental sequences; can misclassify highly similar true variants.

<b>Method/Study</b>	<b>Scope/Approach</b>	<b>Limitations</b>
UCHIME	Alignment-based chimera detection; segments query sequence, identifies parent candidates, performs 3-way alignment, and computes chimera scores; supports both reference-based and de novo modes.	Accuracy inflated in original benchmarks; suffers under incomplete databases; poor performance on low-divergence chimeras; sensitive to sequencing errors; misclassifies when parents are missing.
UCHIME2	Improved uncertainty handling; classifies ambiguous sequences as unknown; offers multiple sensitivity/specifity modes; more robust with incomplete references; higher sensitivity (93–99%).	Cannot achieve perfect accuracy due to “perfect fake models”; genuine variants may be indistinguishable from artificial recombinants; theoretical detection limit remains.
CATCh	First ML ensemble tool for 16S chimera detection; integrates outputs of UCHIME, ChimeraSlayer, DECIPHER, Pintail, Perseus via SVM classifier; significantly improves sensitivity and specificity.	Depends on performance of underlying tools; ML model limited to features they output; ensemble can still misclassify in datasets with extreme novelty or low coverage.

Method/Study	Scope/Approach	Limitations
ChimPipe	Pipeline for detecting fusion genes and transcript-derived chimeras in RNA-seq; uses discordant paired-end reads and split-alignments; predicts isoforms and breakpoint coordinates.	Designed for RNA-seq, not amplicons; needs high-quality genome and annotation; computationally heavier; limited to organisms with reference genomes.
Machine-Learning Sequence Quality & Chimera Detection (general)	Uses k-mer profiles, GC content shifts, entropy, split-read statistics, mapping quality variation, and micro-homology signatures as predictive features; identifies subtle artifacts missed by heuristics.	Requires labeled training data; model performance depends on feature engineering; may capture dataset-specific biases; limited generalization if training data is narrow or unrepresentative.

473 Across existing studies, no single approach reliably detects all forms of chimeric  
 474 sequences, particularly those generated by PCR-induced template switching in  
 475 mitochondrial genomes. Reference-based tools perform poorly when parental se-  
 476 quences are absent; de novo methods rely strongly on abundance assumptions;  
 477 alignment-based systems show reduced sensitivity to low-divergence chimeras; and  
 478 ensemble methods inherit the limitations of their component algorithms. RNA-  
 479 seq-oriented pipelines likewise do not generalize well to organelle data. Although  
 480 machine learning approaches offer promising feature-based detection, they are  
 481 rarely applied to mitochondrial genomes and are not trained specifically on PCR-

482 induced organelle chimeras. These limitations indicate a clear research gap: the  
483 need for a specialized, feature-driven classifier tailored to mitochondrial PCR-  
484 induced chimeras that integrates k-mer composition, split-alignment signals, and  
485 micro-homology features to achieve more accurate detection than current heuristic  
486 or alignment-based tools.

# <sup>487</sup> Chapter 3

## <sup>488</sup> Research Methodology

<sup>489</sup> This chapter outlines and explains the specific steps and activities to be carried  
<sup>490</sup> out in completing the project.

### <sup>491</sup> 3.1 Research Activities

<sup>492</sup> As illustrated in Figure 3.1, the researchers will carry out a sequence of compu-  
<sup>493</sup> tational procedures designed to detect PCR-induced chimeric reads in mitochon-  
<sup>494</sup> drial genomes. The process begins with the collection of mitochondrial reference  
<sup>495</sup> sequences from the NCBI database, which will serve as the foundation for gener-  
<sup>496</sup> ating simulated chimeric reads. These datasets will then undergo bioinformatics  
<sup>497</sup> pipeline development, which includes alignment, k-mer extraction, and homology-  
<sup>498</sup> based filtering to prepare the data for model construction. The machine-learning  
<sup>499</sup> model will subsequently be trained and tested using the processed datasets to  
<sup>500</sup> assess its accuracy and reliability. Depending on the evaluation results, the model

501 will either be refined and retrained to improve performance or, if the metrics meet  
502 the desired threshold, deployed for further validation and application.

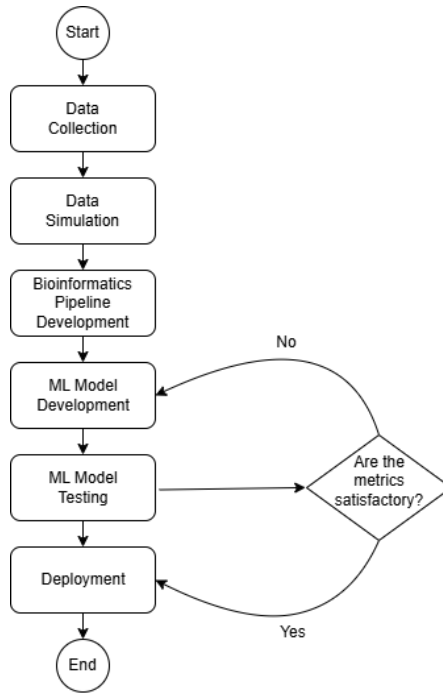


Figure 3.1: Process Diagram of Special Project

### 503 3.1.1 Data Collection

504 The researchers will collect mitochondrial genome reference sequences of *Sar-*  
505 *dinella lemuru* from the National Center for Biotechnology Information (NCBI)  
506 database. The downloaded files will be in FASTA format to ensure compatibility  
507 with bioinformatics tools and subsequent analysis. The gathered sequences will  
508 serve as the basis for generating simulated chimeric reads to be used in model  
509 development.

510 The expected outcome of this process is a comprehensive dataset of *Sardinella*

511 *lemuru* mitochondrial reference sequences that will serve as the foundation for  
512 the succeeding stages of the study. This step is scheduled to start in the first  
513 week of November 2025 and is expected to be completed by the last week of  
514 November 2025, with a total duration of approximately one (1) month.

### 515 3.1.2 Data Simulation

516 The researchers will simulate sequencing data using the reference sequences col-  
517 lected from NCBI. Using `wgsim`, a total of 5,000 paired-end reads (R1 and R2)  
518 will be generated from the reference genome and designated as clean reads. These  
519 reads will be saved in FASTQ (`.fastq`) format. From the same reference, a Bash  
520 script will be created to deliberately cut and reconnect portions of the sequence,  
521 introducing artificial junctions that mimic chimeric regions. The manipulated  
522 reference file, saved in FASTA (`.fasta`) format, will then be processed in `wgsim`  
523 to simulate an additional 5,000 paired-end chimeric reads, also stored in FASTQ  
524 (`.fastq`) format. The resulting read files will be aligned to the original reference  
525 genome using SAMtools, generating SAM (`.sam`) or BAM (`.bam`) alignment files.  
526 During this alignment process, clean reads will be labeled as “0,” while chimeric  
527 reads will be labeled as “1” in a corresponding CSV (`.tsv`) file.

528 The expected outcome of this process is a complete set of clean and chimeric  
529 paired-end reads prepared for subsequent analysis and model development. This  
530 step is scheduled to start in the first week of November 2025 and is expected  
531 to be completed by the last week of November 2025, with a total duration of  
532 approximately one (1) month.

### 533 3.1.3 Bioinformatics Tools Pipeline

534 The researchers will obtain the necessary analytical features through the devel-  
535 opment and implementation of a bioinformatics pipeline. This pipeline will serve  
536 as a reproducible and modular workflow that accepts FASTQ and BAM inputs,  
537 processes these through a series of analytical stages, and outputs tabular feature  
538 matrices (TSV) for downstream machine learning. All scripts will be version-  
539 controlled through GitHub, and computational environments will be standardized  
540 using Conda to ensure cross-platform reproducibility. To promote transparency  
541 and replicability, the exact software versions, parameters, and command-line ar-  
542 guments used in each stage will be documented. To further ensure correctness  
543 and adherence to best practices, the researchers will consult with bioinformatics  
544 experts in Philippine Genome Center Visayas for validation of pipeline design,  
545 feature extraction logic, and overall data integrity. This stage of the study is  
546 scheduled to begin in the last week of November 2025 and conclude by the last  
547 week of January 2026, with an estimated total duration of approximately two (2)  
548 months.

549 The bioinformatics pipeline focuses on three principal features from the sim-  
550 ulated and aligned sequencing data: (1) supplementary alignment count (SA  
551 count), (2) k-mer composition difference between read segments, and (3) micro-  
552 homology length at potential junctions. Each of these features captures a distinct  
553 biological or computational signature associated with PCR-induced chimeras.

554 **Alignment and Supplementary Alignment Count**

555 This will be derived through sequence alignment using Minimap2, with subsequent  
556 processing performed using SAMtools and `pysam` in Python. Sequencing reads  
557 will be aligned to the *Sardinella lemuru* mitochondrial reference genome using  
558 Minimap2 with the `-ax sr` preset (optimized for short reads). The output will  
559 be converted and sorted using SAMtools, producing an indexed BAM file which  
560 will be parsed using `pysam` to count the number of supplementary alignments  
561 (SA tags) per read. Each read's mapping quality, number of split segments,  
562 and alignment characteristics will be recorded in a corresponding TSV file. The  
563 presence of multiple alignment loci within a single read, as reflected by a nonzero  
564 SA count, serves as direct computational evidence of chimerism. Reads that  
565 contain supplementary alignments or soft-clipped regions are strong candidates  
566 for chimeric artifacts arising from PCR template switching or improper assembly  
567 during sequencing.

568 **K-mer Composition Difference**

569 Chimeric reads often comprise fragments from distinct genomic regions, resulting  
570 in a compositional discontinuity between segments. Comparing k-mer frequency  
571 profiles between the left and right halves of a read allows detection of such abrupt  
572 compositional shifts, independent of alignment information. This will be obtained  
573 using Jellyfish, a fast k-mer counting software. For each read, the sequence will  
574 be divided into two segments, either at the midpoint or at empirically determined  
575 breakpoints inferred from supplementary alignment data, to generate left and right  
576 sequence segments. Jellyfish will then compute k-mer frequency profiles (with  $k =$

577 5 or 6) for each segment. The resulting k-mer frequency vectors will be normalized  
578 and compared using distance metrics such as cosine similarity or Jensen–Shannon  
579 divergence to quantify compositional disparity between the two halves of the same  
580 read. The resulting difference scores will be stored in a structured TSV file.

581 **Micro-homology Length**

582 The micro-homology length will be computed using a custom Python script that  
583 detects the longest exact suffix–prefix overlap within  $\pm 30$  base pairs surround-  
584 ing a candidate breakpoint. This analysis identifies the number of consecutive  
585 bases shared between the end of one segment and the beginning of another. The  
586 presence and length of such micro-homology are classic molecular signatures of  
587 PCR-induced template switching, where short identical regions (typically 3–15  
588 base pairs) promote premature termination and recombination of DNA synthesis  
589 on a different template strand. By quantifying micro-homology, the researchers  
590 can assess whether the suspected breakpoint exhibits characteristics consistent  
591 with PCR artifacts rather than true biological variants. Each read will therefore  
592 be annotated with its corresponding micro-homology length, overlap sequence,  
593 and GC content.

594 After extracting the three primary features, all resulting TSV files will be  
595 joined using the read identifier as a common key to generate a unified feature ma-  
596 trix. Additional read-level metadata such as read length, mean base quality, and  
597 number of clipped bases will also be included to provide contextual information.  
598 This consolidated dataset will serve as the input for subsequent machine-learning  
599 model development and evaluation.

### 600 3.1.4 Machine-Learning Model Development

601 The classification component of MitoChime will employ two ensemble algo-  
602 rithms—Random Forest (RF) and Extreme Gradient Boosting (XGBoost)—to  
603 evaluate complementary learning paradigms. Random Forest applies bootstrap  
604 aggregation (bagging) to reduce model variance and improve stability, whereas  
605 XGBoost implements gradient boosting to minimize bias and capture complex  
606 non-linear relationships among genomic features. Using both models enables a  
607 balanced assessment of predictive performance and interpretability.

608 The dataset will be divided into training (80%) and testing (20%) subsets.  
609 The training data will be used for model fitting and hyperparameter optimization  
610 through five-fold cross-validation, in which the data are partitioned into five folds;  
611 four folds are used for training and one for validation in each iteration. Perfor-  
612 mance metrics will be averaged across folds, and the optimal parameters will be  
613 selected based on mean cross-validation accuracy. The final models will then be  
614 evaluated on the held-out test set to obtain unbiased performance estimates.

615 Model development and evaluation will be implemented in Python (ver-  
616 sion 3.11) using the `scikit-learn` and `xgboost` libraries. Standard metrics  
617 including accuracy, precision, recall, F1-score, and area under the ROC curve  
618 (AUC) will be computed to quantify predictive performance. Feature-importance  
619 analyses will be performed to identify the most discriminative variables contribut-  
620 ing to chimera detection.

### 621    3.1.5 Validation and Testing

622    Validation will involve both internal and external evaluations. Internal validation  
623    will be achieved through five-fold cross-validation on the training data to verify  
624    model generalization and reduce variance due to random sampling. External  
625    validation will be achieved through testing on the 20% hold-out dataset derived  
626    from the simulated reads, which will serve as an unbiased benchmark to evaluate  
627    how well the trained models generalize to unseen data. All feature extraction and  
628    preprocessing steps will be performed using the same bioinformatics pipeline to  
629    ensure consistency and comparability across validation stages.

630       Comparative evaluation between the Random Forest and XGBoost classifiers  
631    will establish which model achieves superior predictive accuracy and computa-  
632    tional efficiency under identical data conditions.

### 633    3.1.6 Documentation

634       Comprehensive documentation will be maintained throughout the study to en-  
635    sure transparency, reproducibility, and scientific integrity. All stages of the re-  
636    search—including data acquisition, preprocessing, feature extraction, model train-  
637    ing, and validation—will be systematically recorded. For each analytical step, the  
638    corresponding parameters, software versions, and command-line scripts will be  
639    documented to enable exact replication of results.

640       Version control and collaborative management will be implemented through  
641    GitHub, which will serve as the central repository for all project files, including  
642    Python scripts, configuration settings, and Jupyter notebooks. The repository

643 structure will follow standard research data management practices, with clear  
644 directories for datasets, processed outputs, and analysis scripts. Changes will be  
645 tracked through commit histories to ensure traceability and accountability.

646 Computational environments will be standardized using Conda, with environ-  
647 ment files specifying dependencies and package versions to maintain consistency  
648 across systems. Experimental workflows and exploratory analyses will be con-  
649 ducted in Jupyter Notebooks, which facilitate real-time visualization, annotation,  
650 and incremental testing of results.

651 For the preparation of the final manuscript and supplementary materials,  
652 Overleaf (LaTeX) will be utilized to produce publication-quality formatting, con-  
653 sistent referencing, and reproducible document compilation. The documentation  
654 process will also include a project timeline outlining major milestones such as  
655 data collection, simulation, feature extraction, model evaluation, and reporting to  
656 ensure systematic progress and adherence to the research schedule.

## 657 3.2 Calendar of Activities

658 Table 3.1 presents the project timeline in the form of a Gantt chart, where each  
659 bullet point corresponds to approximately one week of planned activity.

Table 3.1: Timetable of Activities

Activities (2025)	Nov	Dec	Jan	Feb	Mar	Apr	May
Data Collection and Simulation	• • •						
Bioinformatics Tools Pipeline	• •	• • •	• • •				
Machine Learning Development			• •	• • •	• • •	• •	
Testing and Validation						• •	• • •
Documentation	• • •	• • •	• • •	• • •	• • •	• • •	• • •

# 660 References

- 661 Anderson, S., Bankier, A., Barrell, B., Bruijn, M., Coulson, A., Drouin, J., ...  
662 Young, I. (1981, 04). Sequence and organization of the human mitochondrial  
663 genome. *Nature*, 290, 457-465. doi: 10.1038/290457a0
- 664 Arango, G., Garner, E., Pruden, A., Heath, L., Vikesland, P., & Zhang, L. (2018,  
665 02). Deeparg: A deep learning approach for predicting antibiotic resistance  
666 genes from metagenomic data. *Microbiome*, 6. doi: 10.1186/s40168-018  
667 -0401-z
- 668 Bentley, D. R., Balasubramanian, S., Swerdlow, H. P., Smith, G. P., Milton, J.,  
669 Brown, C. G., ... Smith, A. J. (2008). Accurate whole human genome  
670 sequencing using reversible terminator chemistry. *Nature*, 456(7218), 53–  
671 59. doi: 10.1038/nature07517
- 672 Bi, C., Shen, F., Han, F., Qu, Y., Hou, J., Xu, K., ... Yin, T. (2024, 01).  
673 Pmat: an efficient plant mitogenome assembly toolkit using low-coverage  
674 hifi sequencing data. *Horticulture Research*, 11(3), uhae023. Retrieved  
675 from <https://doi.org/10.1093/hr/uhae023> doi: 10.1093/hr/uhae023
- 676 Boore, J. L. (1999). Animal mitochondrial genomes. *Nucleic Acids Research*,  
677 27(8), 1767–1780. doi: 10.1093/nar/27.8.1767
- 678 Cameron, S. L. (2014). Insect mitochondrial genomics: Implications for evolution

- 679 and phylogeny. *Annual Review of Entomology*, 59, 95–117. doi: 10.1146/  
680 annurev-ento-011613-162007
- 681 Dierckxsens, N., Mardulyn, P., & Smits, G. (2017). Novoplasty: de novo assembly  
682 of organelle genomes from whole genome data. *Nucleic Acids Research*,  
683 45(4), e18. doi: 10.1093/nar/gkw955
- 684 Edgar, R. C. (2016). Uchime2: improved chimera prediction for amplicon se-  
685 quencing. *bioRxiv*. Retrieved from <https://api.semanticscholar.org/>  
686 CorpusID:88955007
- 687 Edgar, R. C. (n.d.). Uchime in practice. Retrieved from [https://www.drive5.com/usearch/manual7/uchime\\_practical.html](https://www.drive5.com/usearch/manual7/uchime_practical.html)
- 688
- 689 Edgar, R. C., Haas, B. J., Clemente, J. C., Quince, C., & Knight, R. (2011).  
690 Uchime improves sensitivity and speed of chimera detection. *Bioinformatics*,  
691 27(16), 2194–2200. doi: 10.1093/bioinformatics/btr381
- 692 Frenkel-Morgenstern, M., Lacroix, V., Ezkurdia, I., Levin, Y., Gabashvili, A.,  
693 Prilusky, J., ... Valencia, A. (2012, 05). Chimeras taking shape: Potential  
694 functions of proteins encoded by chimeric rna transcripts. *Genome research*,  
695 22, 1231-42. doi: 10.1101/gr.130062.111
- 696 Glenn, T. C. (2011). Field guide to next-generation dna sequencers. *Molecular  
697 Ecology Resources*, 11(5), 759–769. doi: 10.1111/j.1755-0998.2011.03024.x
- 698 Gonzalez, J. M., Zimmermann, J., & Saiz-Jimenez, C. (2004, 09). Evalu-  
699 ating putative chimeric sequences from pcr-amplified products. *Bioin-  
700 formatics*, 21(3), 333-337. Retrieved from <https://doi.org/10.1093/bioinformatics/bti008> doi: 10.1093/bioinformatics/bti008
- 701
- 702 Gray, M. W. (2012). Mitochondrial evolution. *Cold Spring Harbor perspectives  
703 in biology*, 4. Retrieved from <https://doi.org/10.1101/cshperspect.a011403> doi: 10.1101/cshperspect.a011403
- 704

- 705 Hahn, C., Bachmann, L., & Chevreux, B. (2013). Reconstructing mitochondrial  
706 genomes directly from genomic next-generation sequencing reads—a baiting  
707 and iterative mapping approach. *Nucleic Acids Research*, 41(13), e129. doi:  
708 10.1093/nar/gkt371
- 709 Jin, J.-J., Yu, W.-B., Yang, J., Song, Y., dePamphilis, C. W., Yi, T.-S., & Li,  
710 D.-Z. (2020). Getorganelle: a fast and versatile toolkit for accurate de  
711 novo assembly of organelle genomes. *Genome Biology*, 21(1), 241. doi:  
712 10.1186/s13059-020-02154-5
- 713 Judo, M. S. B., Wedel, W. R., & Wilson, B. H. (1998). Stimulation and sup-  
714 pression of pcr-mediated recombination. *Nucleic Acids Research*, 26(7),  
715 1819–1825. doi: 10.1093/nar/26.7.1819
- 716 Labrador, K., Agmata, A., Palermo, J. D., Ravago-Gotanco, R., & Pante, M. J.  
717 (2021). Mitochondrial dna reveals genetically structured haplogroups of  
718 bali sardinella (sardinella lemuru) in philippine waters. *Regional Studies in*  
719 *Marine Science*, 41, 101588. doi: 10.1016/j.rsm.2020.101588
- 720 Layer, R., Hall, I., & Quinlan, A. (2014, 10). Lumpy: A probabilistic framework  
721 for structural variant discovery. *Genome Biology*, 15. doi: 10.1186/gb-2014  
722 -15-6-r84
- 723 Li, H. (2018, 05). Minimap2: pairwise alignment for nucleotide sequences. *Bioin-*  
724 *formatics*, 34(18), 3094-3100. Retrieved from <https://doi.org/10.1093/bioinformatics/bty191>  
725 doi: 10.1093/bioinformatics/bty191
- 726 Liang, Q., Bible, P. W., Liu, Y., Zou, B., & Wei, L. (2020, 02). Deepmi-  
727 crobes: taxonomic classification for metagenomics with deep learning. *NAR*  
728 *Genomics and Bioinformatics*, 2(1), lqaa009. Retrieved from <https://doi.org/10.1093/nargab/lqaa009>  
729 doi: 10.1093/nargab/lqaa009
- 730 Metzker, M. L. (2010). Sequencing technologies — the next generation. *Nature*

- 731        *Reviews Genetics*, 11(1), 31–46. doi: 10.1038/nrg2626
- 732    Mysara, M., Saeys, Y., Leys, N., Raes, J., & Monsieurs, P. (2015). Catch,  
733        an ensemble classifier for chimera detection in 16s rrna sequencing stud-  
734        ies. *Applied and Environmental Microbiology*, 81(5), 1573-1584. Retrieved  
735        from <https://journals.asm.org/doi/abs/10.1128/aem.02896-14> doi:  
736        10.1128/AEM.02896-14
- 737    Qin, Y., Wu, L., Zhang, Q., Wen, C., Nostrand, J. D. V., Ning, D., ... Zhou, J.  
738        (2023). Effects of error, chimera, bias, and gc content on the accuracy of  
739        amplicon sequencing. *mSystems*, 8(6), e01025-23. Retrieved from <https://journals.asm.org/doi/abs/10.1128/msystems.01025-23> doi: 10.1128/  
740        msystems.01025-23
- 741    Qiu, X., Wu, L., Huang, H., McDonel, P. E., Palumbo, A. V., Tiedje, J. M., &  
742        Zhou, J. (2001). Evaluation of pcr-generated chimeras, mutations, and het-  
743        eroduplexes with 16s rrna gene-based cloning. *Applied and Environmental  
744        Microbiology*, 67(2), 880–887. doi: 10.1128/AEM.67.2.880-887.2001
- 745    Ren, J., Song, K., Deng, C., Ahlgren, N., Fuhrman, J., Li, Y., ... Sun, F. (2020,  
746        01). Identifying viruses from metagenomic data using deep learning. *Quan-  
747        titative Biology*, 8. doi: 10.1007/s40484-019-0187-4
- 748    Rodriguez-Martin, B., Palumbo, E., Marco-Sola, S., Griebel, T., Ribeca, P.,  
749        Alonso, G., ... Djebali, S. (2017, 01). Chimpipe: Accurate detection of  
750        fusion genes and transcription-induced chimeras from rna-seq data. *BMC  
751        Genomics*, 18. doi: 10.1186/s12864-016-3404-9
- 752    Rognes, T., Flouri, T., Nichols, B., Quince, C., & Mahé, F. (2016). Vsearch: a  
753        versatile open source tool for metagenomics. *PeerJ*, 4, e2584. doi: 10.7717/  
754        peerj.2584
- 755    Sedlazeck, F., Rescheneder, P., Smolka, M., Fang, H., Nattestad, M., von Haeseler,

- 757 A., & Schatz, M. (2018, 06). Accurate detection of complex structural  
758 variations using single-molecule sequencing. *Nature Methods*, 15. doi: 10  
759 .1038/s41592-018-0001-7
- 760 Sfeir, A., & Symington, L. S. (2015). Microhomology-mediated end joining: A  
761 back-up survival mechanism or dedicated pathway? *Trends in Biochemical  
762 Sciences*, 40(11), 701-714. Retrieved from <https://www.sciencedirect.com/science/article/pii/S0968000415001589> doi: <https://doi.org/10.1016/j.tibs.2015.08.006>
- 765 Vervier, M. P. T. M. V. J. B. . V. J. P., K. (2015). Large-scale machine learning  
766 for metagenomics sequence classification. *Bioinformatics*, 32, 1023 - 1032.  
767 Retrieved from <https://api.semanticscholar.org/CorpusID:9863600>
- 768 Willette, D., Bognot, E., Mutia, M. T., & Santos, M. (2011). *Biology and ecology  
769 of sardines in the philippines: A review* (Vol. 13; Tech. Rep. No. 1). NFRDI  
770 Technical Paper Series. Retrieved from <https://nfrdi.da.gov.ph/tpjf/etc/Willette%20et%20al.%20Sardines%20Review.pdf>
- 771